Heliyon 10 (2024) e24284

Contents lists available at ScienceDirect

Heliyon

journal homepage: www.cell.com/heliyon

Research article

Physicochemical and pharmacotechnical characterization of Prussian blue for future Prussian blue oral dosage forms formulation

Borja Martínez-Alonso [a], Norma S. Torres Pabón [a], María Isabel Fernández-Bachiller [b], Guillermo Torrado Durán [a], Rocío González Crespo [a], Carlos F. Torrado-Salmerón [c], Antonio Juberías Sánchez [d], M. Ángeles Peña Fernández [a,*]

[a] Department of Biomedical Sciences, University of Alcalá (UAH), Spain
[b] Center for Applied Chemistry and Biotechnology (CQAB), University of Alcalá (UAH), Spain
[c] Department of Pharmaceuticals and Food Technology, Complutense University of Madrid (UCM), Spain
[d] Defending Pharmacy Military Center, Spain

ARTICLE INFO

Keywords:
Antidote
Prussian blue
Cesium
Characterization
Decorporation
Radionuclide
Thallium

ABSTRACT

Ferric hexacyanoferrate, Fe_4 $[Fe(CN)_6]_3 \cdot xH_2O$, known as Prussian blue (PB), has proven its effectiveness as an antidote in cases of accidental poisoning or poisoning caused by radioactive materials such as cesium (Cs) and thallium (Tl); which due to their solubility in water, when absorbed by the human body, cause serious damage to vital organs. The local development of a drug with PB as an active ingredient arises as a response to the civil and military needs established within the Ministry's pharmacy request for national defense. This fact contemplates the circumstances related to public health protection in the nuclear, radiological, biological and chemical (NRBQ) of the emergency institutions in health and national security. In this paper and by using various analytical techniques, the characterization of the locally synthesized PB with pharmaceutical quality has been described, as a first step to predict its behavior in the preparation of a drug that contains it as an active ingredient.

The research findings demonstrate that locally synthesized PB is suitable for use in oral dosage forms, enabling the local development of drug formulations incorporating PB, thus being able to potentially become a main resource in the treatment of Cs and Tl poisoning in any accidental or intended of the population. This development opens up the possibility of creating drug formulations that incorporate PB at a local level, making it a potentially significant resource in the treatment of Cs and Tl poisoning. The ability to locally produce and utilize PB in oral dosage forms could be crucial in addressing cases of accidental or intentional exposure within the population. This advancement not only contributes to the scientific understanding of PB but also holds promising implications for practical applications in public health and emergency situations.

* Corresponding author.
E-mail addresses: bor-ja.martineza@edu.uah.es (B. Martínez-Alonso), isabel.fernandez@fgua.es (M.I. Fernández-Bachiller), ctorrado@ucm.es (C.F. Torrado-Salmerón), fjuberias@yahoo.es (A.J. Sánchez), angeles.pena@uah.es (M.Á. Peña Fernández).

https://doi.org/10.1016/j.heliyon.2024.e24284
Received 10 August 2023; Received in revised form 3 January 2024; Accepted 5 January 2024
Available online 8 January 2024

1. Introduction

Within the strategic plans for national security and health control in any part of the world, it is a priority to have a technology that allows the availability of resources for the protection of the safety of its citizens in the quality, quantity and time that is required [1].

A wide variety of public health topics, like the ones in the different plans for national security and health control, are in continual development with the objective of preventing and responding to potential hazards for people's health. From its origins in the field of carcinogenic substances [2,3]; going through matters such as control in epidemiologic diseases or climatic and weather effects over health [4,5], to those more recent global problems which has conditioned entire countries efforts to overcome them, we are talking about the COVID-19 pandemic [6,7] and the still present war of Ukraine and Russia [8].

In all of these scenarios the main objectives and general courses of action are common: prevention and identification of risk factors to avoid diseases, improving the health conditions of the population, being prepared to act in case of necessity in the most efficient way and learning from the experience acquired in the situations where the public health have been compromised [9,10].

One of the menaces for public health, is the possible exposition to radiation or toxic related materials, as a consequence it is well known that, at a global level, strategical projects have emerged to act proactively in guaranteeing the availability of material and technological resources specifically designed to counteract foreseeable damages in exposed subjects, to minimize the long-term effects, as well as, if necessary, to provide a constant supply up to have controlled the risky situations [1,11–16].

Such projects are of crucial importance for developed countries or those regions in which their population could be exposed accidently or intentionally to radioactive and/or highly toxic materials such as cesium (Cs) and thallium (Tl) from military or terrorist origin.

A radioisotope, radionuclide, radioactive nuclide, or radioactive isotope is the term to designate an atom that has an excess of nuclear energy, which makes it unstable, transforming it into more stable forms of this atom with the release of ionizing radiation. The period elapsed until half of the atom reaches its non-radioactive form is called the half-life time ($t_{1/2}$), which is characteristic of each specie and can range from fraction of a second to thousands of years [17,18].

Radionuclides can be naturally occurring, as in the case of uranium, but they can also be manufactured, such as Cs. Natural Cs is present in the environment only in a stable form, the isotope ^{133}Cs. The radioactive forms of Cs (^{134}Cs and ^{137}Cs) are produced by fission of uranium in nuclear plants or when nuclear weapons are detonated and degenerate to their stable forms producing beta particles and gamma radiation that have detrimental effects on health. The half-life of radioactive Cs is around 2 years for ^{134}Cs and 30 years for ^{137}Cs [17,19].

It has been reported that the harmful effects on human health by body loads of ^{137}Cs that have entered the body, inhaled, orally or through open wounds, can be either immediate and fatal, or manifest up to years after exposure as cases of cancer, and even as inherited disorders. Tl poisoning is usually caused by accidently or intentionally ingesting the non-radioactive form of this element [12,20–24].

The various clinical cases that are documented report that the difficulty of early diagnosis influences the speed with which the patient's health deteriorates, the severity and irreversibility of multi-organ and systemic effects, which in some cases lead to death of the patient [15,18,20,21,24,25].

Current therapies for radiological exposures intoxications are based in the treatment of the acute radiation syndrome, in others word, most of the treatment is focused on reducing the effects of radiation on the body and a posterior treatment for the consequences of the acute radiation syndrome, like for example, granulocyte colony-stimulating factor. There are only a few treatments eliminating or impeding the action of the font of radiation, or more accurately, countermeasures for radioisotope-specific toxicities, some of them, like potassium iodide impede the union of the radioactive iodide to the thyroid gland, by saturating it; or compounds with decorporant capacity, like Zn/Ca diethylene triamine pentaacetic acid, for plutonium contamination or Prussian blue (PB) for Cs and Tl [26–28].

Decorporation is the term used to refer to the treatment of reducing, by complexation, part of the body burden of the radionuclide or of the toxin using substances proven effective for this purpose, such as PB [2,23,29,30].

1.1. Prussian blue as a decorporating agent

Insoluble PB or ferric hexacyanoferrate is a dark blue pigment, whose formula is Fe_4 $[Fe(CN)_6]_3 \cdot x\ H_2O$ (x = 14–16) (Fig. 1), in

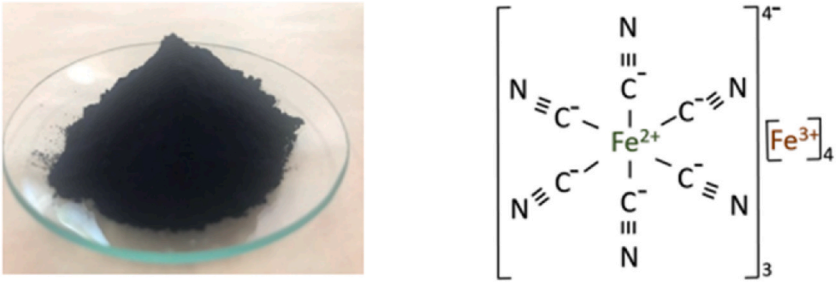

Fig. 1. PB, Fe4 [Fe(CN)6]3 · xH2O (x = 14–16).

which transition metal ions are assembled through cyano-bridges, generating a cubic lattice with a face-centered cubic unit cell alternating Fe^{2+} and Fe^{3+} cations bridged by cyanides, which alternately coordinate to form a cubic unit cell. Thus, chemically it is a species coordinated with a basic cubic lattice centered on the face with iron +3 (Fe^{+3}), octahedrally bound to 6 nitrogen (N) and iron atoms +2 (Fe^{+2}) bonded to 6 carbon atoms ™ of the cyanide ion (CN^{-1}).

PB must not be confused nor being contaminated with the soluble form of the species which responds to the formula K_4Fe_4 [$Fe(CN)_6]_4$ named as potassium hexacyanoferrate compound. This species is not approved by FDA as a decorporant agent for radioactive Cs or Tl and must be always avoided [16,18,31].

PB is a porous organometallic compound, from the group of Metal Organic Frameworks (MOFs), which corresponds to crystalline and porous metal-organic solids formed by the coordinated covalent union of metal ions or clusters and organic molecules, called ligands, giving rise to neutral molecules. These materials are characterized by having large pore volumes and the highest surface areas known to date [31,32].

Zeolites are crystalline materials with a structure of small regular pores that allow molecules to enter their interior. PB is known for its zeolitic character, because it acts as a molecular sieve and/or ion exchanger, due to the open structure of its crystal lattice and therefore it is capable of harbouring not only small molecules of water but also metal ions such as Cs and Tl, among others.

PB has been effectively used for the treatment of patients contaminated with radioactive cesium, ^{137}Cs, radio-active thallium, ^{201}Tl, or in clinical situations of patients with non-radioactive Tl poisoning. PB can reduce the bio-logical half-life of Cs from around 110 to 30 days, in the case of Tl from 8 to 3 days, and therefore it diminishes exposure to the harmful effects of these substances in the same proportions. Due to its ability to decorporate at the intestinal level, PB greatly reduces the amount in which harmful substances are reabsorbed by the body at this level, thus being eliminated in the fecal matter [16,18,20,31,33].

The Cs and Tl ions are very soluble in water and their biological behavior profiles are similar to those of potassium and sodium, so their effects are widely distributed once they enter the body where they act balancing the electrical charges between the interior and exterior of muscle and nerve cells. The kidney purifies part of these elements from the blood by eliminating them in the urine, another part is excreted in the feces and the rest re-mains in the body causing the acute and long-term characteristic effects of each element [33]. The sooner toxic substance circulating is decorporated, the less will be the amount and severity of their damaging effects on the body [34–36].

The decorporation treatment of an adult patient for both cases is oral, with a pattern that is between 200 and 350 mg/kg/day (in three doses, for a total between 1200 and 3000 mg/day), which depends on many factors such as the route of exposure, the initial charge concentration in the body, the pati'nt's previous health status and the physicochemical properties of the harmful element, among which its solubility, particle size and pH stand out, but mainly the lapse of time between exposure and the start of decorporation therapy [22,31,37].

As the possibility of avoiding or mitigating the harmful effects on health in the long term with decorporation therapy is very limited, the term "urgent approach" arises, which consists of starting the treatment of all victims with suspected contamination as quickly as possible, until they have been formally excluded from said risk, by measuring the relevant contamination [12,14,21,24,25].

Currently, there is only one drug with PB approved by the FDA, which was developed to be available for use by first responders in the North American territory given the national security background and to respond to fortuitous events, risks of war events and/or bioterrorism [6,7,33].

Following the North American example, and considering that PB is a costly drug which is not be easily available as a pharmaceutical grade chemical, the Spanish Defense Ministry, in order to guarantee the Spanish national security and its capacity of response in view of the different risks, involving radioactive Cs an Tl, above mentioned; created a project for the development of a locally synthesized PB drug.

This project is known as the AZPINDECs proje"t "Development of a pharmaceutical formula for oral use that allows the use of PB as an agent for the decorporation of ^{137}Cs and other radioactive and toxic spec"es", in which the University of Alcalá (UAH), the Complutense University of Madrid (UCM) and the Defending Pharmacy Military Center (CEMILFARDEF) works together in order to give a response to the need for local availability of treatment for subjects accidently or intentionally exposed to these materials, in the quality and quantity that al-low the control of this risk effectively in the Spanish territory.

1.2. Pharmaceutical forms for oral use

The development of medicines starts from the study of the active ingredient, taking into account the needs of the user and the technological possibilities. Within the diversity of pharmaceutical forms, those for oral administration are usually one of the most frequently adopted due to the ease of administration of different doses of active ingredient(s) and follow-up of the treatment and, on the other hand, due to the know-how with which it is available for all the operations involved in its elaboration from development scale to the different sizes of industrial level [38,39].

Due to the insolubility properties of PB, solid pharmaceutical forms for oral administration are the ones which suits the most, among the variety of oral pharmaceutical forms, for the development of a new PB formulation.

Tablets are the pharmaceutical form that best meet the characteristics described above. Among the main technological advantages that justify the frequent choice of tablets as a pharmaceutical form for oral use are the availability of machinery and equipment for their development and elaboration at different scales of production and control in any pharmaceutical production plant, and its possibility supply in the quantity demanded, attending to the different needs established during the formulation design, quickly and economically.

The manufacture of tablets is characterized by the compression of a pulverulent mixture or a granulate. They may contain one or

more active ingredients, and the addition of several excipients is usually necessary, especially when compared to the number of excipients needed to formulate other solid forms, such as capsules. Because of this, is mandatory to establish the physicochemical and pharmacotechnical properties of PB [40,41].

The aim of this study is to characterize the locally synthesized PB, determine if it is similar to the reference PB used in the authorized drug Radiogardase® and analyze its qualities for a future formulation in oral tablets. Therefore, to meet all these points, this work aims to study the physicochemical and pharmacotechnical properties of local PB and compare them with those of standard PB. All this focused on the rationale of the AZPINDECs project, which is the development of an oral pharmaceutical form with PB as an active pharmaceutical ingredient, so that the national supply capacity of this medicine is guaranteed in case of need.

In addition, arises a secondary objective, through the determination of these physicochemical and pharmacotechnical properties, to develop the ability to establish the difference between the PB approved for it use as a drug and other chemicals forms of PB which are not authorized, by using the analytical techniques described in this study.

2. Materials and methods

Studies of elemental analysis (EA), Scanning Electronic Microscopy (SEM), Laser Diffraction Technology for Measuring Particle Size Distributions (PSDs), angle of repose, Differential Scanning Calorimetry (DSC), Fourier Transform Infrared Spectrophotometry (FTIR), Thermogravimetric Analysis (TGA) and X-Ray Diffraction (XRD) were made.

2.1. Locally developed PB and standard PB

The PB used in these studies was locally developed in the Center for Applied Chemistry and Biotechnology (CQAB) from the UAH. Its physicochemical and pharmacotechnical properties needed for this study were determined on the batch DFO-2009-083 DPE. For obtaining PB as an active principle, the direct synthetic pathway was applied. Basically, the direct method consists in one-step process in which an excess of solution of an iron (II) salt is mixing with a solution of hexacyanoferrate (II) salt. The deep blue precipitate is filtered and carefully washed with distilled water [42].

The PB used as a standard for comparison whit the local™oped PB was the PB contained in the capsules of Radiogardase®-Cs 500 mg hardcapsules, batch number 24002125. Radiogardase®-Cs 500 mg hardcapsules is the only drug containing PB as an active authorized [31]. Three different commercially available PB from separated suppliers were also used as an additional source for comparison and thus, for obtaining more valuable data in various analysis. The first commercial PB (PB1) was purchased from Liuyang Donghao Warehousing (Chang-sha-Liuyang, China), the second commercial PB (PB2) was purchased from Haihang industry Co. (Jinan, China) whereas the third was purchased from Sigma Aldrich (CAS Number: 14,038-43-8), named as PB3.

It must be noted that these two commercial PB (PB1 and PB2) are not accompanied by a certificate of analysis that guarantees their chemical composition as ferric hexacyanoferrate, existing therefore the possibility of being contaminated by soluble species.

2.2. Elemental analysis (EA)

A CHNS test was performed in an elemental analyzer LECO CHNS-932 (LECO, United States) to stablish the average weight of C, H and N in the samples of locally developed PB, referred as PB test, in comparison with the Radiogardase® PB standard. Also, PB1 and PB2 samples were analyzed and compared with PB standard and PB test [43].

2.3. Scanning Electronic Microscopy (SEM)

The appearance and shape of the particles of PB test and PB standard were determined by an electron micro-scope Hitachi 15 KV tabletop microscope (Japan).

Crystals are solids composed of atoms arranged in a three-dimensional periodic pattern. SEM studies are carried out to study the surface morphology of different types of particles. The samples were prepared by fixing them to a sample holder and covering them with fine metallic particles using the techni“ue called “sputtering”, which consists of covering the samples in a cathode evaporator with a thin layer of gold particles, between 10 and 25 nm approximately. In this way, the light beams that impact on its surface are reflected differentially according to their morphology, providing very precise information on the shape and dimensions of the surface, at different magnifications [28,29]. The observations were made for all cases with an acceleration voltage of 15 kV after adhering the powder to the sample holder.

2.4. Particle size distribution studies (PSDs)

To characterize the particle size of both PB standard and PB test, a granulometric study was performed by using the analyzer Mastersizer 3000 Hydro EV from Malvern Inc (Malvern Panalytical, Almelo, Netherlands), which uses laser diffraction technology. The particle size was determined using wet method and water as dispersant (Refractive Index: 1.330). The parameters considered in these experiments were: sample measurement time of 5.00 s and a stirring speed of 2100 rpm. Due to the hydrodynamic radius that DLS measures depends strongly on the particle morphology, to determine the particle size the Mie theory, which considers the particles as spheres, was applied. In this case, the particle refractive index value of PB was 1.560. The analysis is recorded in number/volume distribution.

2.5. Angle of repose determination

The determination of the angle of repose for PB test was carried out following the method described on the Real Farmacopea Española [44].

For the test a funnel was placed perpendicularly on a flat surface at a distance of 20 cm of the table from the bottom of the funnel. In all experiments, 10 g of PB test were placed in the funnel blocking the exit, after placed it was let to fall completely over the flat surface.

The average of the two perpendicular diameters of the pile of material and the height are measured in triplicate. Under these conditions, the angle of repose is determined by calculating its tangent, as follows:

$$\alpha^{\circ} = arc\ tg\ \frac{h\ (cm)}{r^{'}(cm)}$$

where α° is the angle of repose, h is the maximum height reached by the dust, measured in centime'ers, and r', also in centimeters, results from the calculation of the corrected average diameter, which is determined by subtracting from the diameter occupied by the material the diameter of the stem opening of the funnel used for the determination.

2.6. Differential Scanning Calorimetry (DSC)

The DSC measurements for PB test and PB standard were performed in a Mettler TA 4000 DSC Star System instrument (Switzerland), using a temperature range from 25 °C to 250 °C, with a heating ratio of 5 °C/min. Samples were accurately weighed (4 mg) into aluminum sealed pans. The equipment was calibrated for baseline and temperature with indium metal.

2.7. Fourier Transform Infrared Spectrophotometry (FTIR)

The Infra-Red spectra of all PB considered in this study were recorded by using the instrument Fourier Spectrum 2000 spectrometer PerkinElmer® System 20000FT-IR (United States).

For samples preparation, 2.5 mg of the corresponding PB (test, standard, PB1 or PB2) were weighted, and KBr (Panreac Química S. L.U., Barcelona, Spain), transparent to infrared radiation, was added until a total of 250 mg was reached. Both raw materials were mixed in an agate mortar until a complete mixture with adequate particle size is reached. Then, the mixture was pressed into a tablet, applying a force of 10 tons for 15 s. The Infrared spectra were recorded performing ten scans in wavelengths range from 4000 to 400 cm^{-1}.

2.8. Thermogravimetric analysis (TGA)

The variation of the weight of a sample as a function of temperature was determined by thermogravimetric analysis using the TA Instruments GA55 TGA Analyzer (United States of America). The heating was 20 °C/min starting from 25 °C to 360 °C with a N_2 flow of 40 mL/min. This technique provides information about both water content and thermal stability [45].

2.9. X-ray diffraction (XRD)

To carry out the characterization of the PB test, the method of powder and surface sweep was used with a Philips® X'Pert-MPD X-ray diffractometer (Malvern Panalytical, Almelo, Netherlands). The sample is placed on a sample holder, and it is impacted with monochromatized CuKα radiation. The conditions established for this test were 40 KV of voltage and 55 mA of intensity. The diffractograms obtained from the PB test allow to know its degree of relative crystallinity, by comparing the intensity of the signal obtained against PB standard.

2.10. Determination of metal composition by inductively coupled plasma mass spectrometry (ICP-MS)

2.10.1. Analytical method and validation

All samples PB samples were analyzed by inductively coupled plasma mass spectrometry (ICP-MS) using a ICP-MS (7700x, Agilent Technologies). Each sample was analyzed in triplicate. Blanks were run between every sample. Standard regression lines were obtained as the mean of three injections of each calibration point, and the regression coefficient was >0.99. The concentration ranges used in the regression lines were 5–1000 ng/L and 0.005–1000 μg/L in 1 % nitric acid for Hg and the rest of metals, respectively. The samples were prepared in different ways using two sampling protocols.

Solid samples were subjected to a microwave (ETHOS One, Millestone) digestion process using a mixture of HNO3: HCl (1:3) and applying a temperature ramp up to 190 °C. After that, the samples were filtered out through PVDF filters (0.45 μm). The digested extract was put in a flask and diluted with ultrapure water (100 mL). For the quantification for Fe, Mg and K, the extracts were subjected to different dilutions (1/5, 1/100, 1/1000) in HCl (1.8 %): HNO3 (0.6 %) medium according to instrumental requirements. The signal instrumental (cps) is interpolated in the corresponding external calibration line, being the linear ranges used: 3 μg/L – 1000 μg/L for Mg and K, and 10 μg/L – 1000 μg/L for Fe. ICP instrument conditions were: Forward power: 1550 W; Gas plasma flow: 15 L/min; Carrier gas flow: 1.10 L/min; collision gas: He; Collision gas flow: 4.3 mL/min; Integration time: 100 ms in triplicate.

Liquid samples were acidified with HNO3 (−9%) (pH 2–3) and filtered out using PVDF syringe filters with a pore size of 0.45 μm. Then, they were applied for serial dilutions (1/10, 1/200, 1/2000) in HNO3 medium (1 %) according to the instrumental requirements. The content of Cs and K was quantified by external calibration interpolating the instrumental signal (cps) within the linear intervals 1 μg/L – 10 mg/L and 3 μg/L – 1 mg/L for Cs and K, respectively.

2.10.2. Determination of Cs binding capacity at pH 7.4 for 24 h (600 ppm)

A 0.1 g amount of each PB was introduced individually to a glass flask (100 mL). After that, a phosphate buffer solution of 40 mM with pH 7.4 and Cs stock solution (30 mg/mL Cs) was added, resulting in a final concentration of 600 ppm. The flask was tightly closed and incubated in a shaking bath at 37 °C with 40 shakes/min for 24 h. All sample batches were prepared in triplicate. After this incubation process, the samples were filtered out with 0.2 μm Acrodisc® syringe filter and then, an aliquot of sample (10 mL) was transferred to a glass test tube. The sample was diluted, if necessary. All the samples were prepared in triplicate. After that, the content of Cs was determined by using the experimental procedure described above for liquid samples.

2.10.3. Concentration profile (600, 750, 900, 1200, 1500, 1800 ppm) at pH 7.4 for 24 h

In phosphate buffer solution 40 mM pH 7.4 (49 mL) and Cs stock solution (30, 37.5, 45, 60, 75 or 90 mg/mL Cs) (1 mL) were added into a glass flash (100 mL), followed by the addition of PB (0.1 g) to produce a final Cs concentration of 300, 600, 750, 900, 1200, 1500 or 1800 ppm. The flash was tightly closed and incubated in a shaking bath at 37 °C with 40 shakes/min for 24 h. After this incubation process, the samples were filtered out with 0.2 μm Acrodisc® syringe filter and then, an aliquot of sample (10 mL) was transferred to a glass test tube. The sample was diluted, if necessary. All the samples were prepared in triplicate. After that, the content of Cs was determined by using the experimental procedure described above for liquid samples.

3. Results and discussion

The locally synthesized PB was characterized by using the following methods and techniques, employing the PB active contained in Radiogardase® as standard. In addition, three commercial samples of PB were subjected to various of these analysis for expanding the knowledge and comparison with both PB standard and the PB test.

3.1. Elemental analysis (EA)

The average of percent of weight of C, H and N obtained for every PB is reported in Table 1. The results of the chemical analysis clearly demonstrate that all the samples have a composition close to the ideal formula Fe_4 $[Fe(CN)_6]_3$. xH_2O corresponding to the stoichiometry of "insoluble PB". Moreover, as can be seen in the results of the EA, the PB test, obtained in the UAH has a composition equivalent to that of the PB standard, which correspond to the formula of the PB and its relative composition with respect to C, H and N.

Considering that the general molecular formula of insoluble PB is Fe_4 $[Fe(CN)_6]_3 \cdot xH_2O$, and that the percent of H is closely related with the water content, the obtained results reveal that the PB standard contains 19 water molecules, whereas the PB obtained by synthesis is characterized by the presence of 18 (Table 1). The differences observed can be attributed to the fact that the exact degree of hydration is unknown and the difficulty of determining it accurately.

Taking in to account the proposed action mechanism for PB in which the zeolitic water contained in the empty spaces of the crystalline lattice is fundamental for the incorporation of the Cs^+ cations, as the space generated by losing the water molecules favours the union of ^{137}Cs due to the similar size of the space and the ^{137}Cs ionic radium; a major amount of water contents, as seen in PB test and PB standard, means an improvement in the decorporant capacity of PB [46].

Regarding to the results obtained for PB1, PB2 and PB3, it can be observed a proportional increase in the percentage of C nd N, as well as a decrease in the percentage of H, which indicates a lower water content in the formula. In function of the obtained percentages, the molecular formula for each PB is depicted also in Table 1 and seem that they contain between 6 and 7 water molecules in their structure. So, the theoretical percentage is calculated in function of these molecular formula. Due to the lower water content is expected that these PB derivatives will have a minor decorporant capacity and can also be an indicator of the soluble form of PB, this is because the increase in N and C is equivalent to the addition of a CN^- group occupying the free space of the unit cell present in the insoluble PB [46].

Table 1
Elemental analysis of PB.

Sample	Molecular Formula	Theoretical			Experimental determined		
		%C	%H	%N	%C	%H	%N
PB1	Fe_4 $[Fe(CN)_6]_3 \cdot 6H_2O$	22.33	1.2	26.05	21.03 ± 0.07	2.05 ± 0.06	26.19 ± 0.05
PB2	Fe_4 $[Fe(CN)_6]_3 \cdot 6H_2O$	22.33	1.2	26.05	21.12 ± 0.37	1.82 ± 0.14	26.77 ± 0.11
PB3	Fe_4 $[Fe(CN)_6]_3 \cdot 6H_2O$	22.33	1.2	26.05	21.03 ± 0.07	2.05 ± 0.06	26.19 ± 0.05
PB standard	Fe_4 $[Fe(CN)_6]_3 \cdot 18H_2O$	18.40	3.1	21.50	18.64 ± 0.21	3.17 ± 0.06	19.58 ± 0.15
PB test	Fe_4 $[Fe(CN)_6]_3 \cdot 22H_2O$	17.20	3.5	20.07	17.49 ± 0.48	3.07 ± 0.03	18.44 ± 0.35

3.2. Thermogravimetric analysis (TGA)

The thermogravimetric analysis has been used to estimate the percentage of water content in all the PBs used. To visualize better the moisture in every sample, the first derivative was represented (Figs. 2 and 3). As it is shown in Fig. 2, in both PB standard and PB test appears the first mass loss, below 180 °C, which corresponds to the evacuation of zeolitic water molecules, whereas the second mass loss appears between 180 °C and 230 °C, which is related to the loss of coordinated water. In the case of PB test, the percentage of weight lost between 25 and 230 °C is 32 %. This loss of weight is attributed to the presence of 22 water molecules in its structure. These results agree with the reported data in which describes that the water content of active pharmaceutical PB as ingredient [47]. These water molecules in PB can be distinguished as either coordination or crystallization. The coordination water molecules are six and are occupying by Fe(III) via the six empty nitrogen (CN) coordination moieties. However, the rest of water molecules or crystallization/zeolitic water molecules are partially connected to the coordination ones via hydrogen bonds and represents between 8 and 12 molecules and are responsible that the PB active ingredient maintenance the Cs binding capacity [48]. However, in the PB standard, the loss of weight in this region is a smaller (27 %). This result indicates that PB standard contains 18 water molecules. These results agree with those obtained by elemental analysis. Weight loss above 250 °C was due to the decomposition of C–N bindings.

The TGA curves of PB1, PB2 and PB3 (Fig. 3) show low loss of weight below 180 °C (in the range of 3.47–3.57), indicating that both products have few zeolitic water molecules in their crystalline network, also, while the water lost below 180 °C is lower, the total loss of weigh is similar to that of PB standard and test, meaning that PB1 and PB2 have a higher weigh lost over 230 °C, which corresponds to a dramatic loss of CN- groups from the molecule and, therefore, the lower water content in their structures makes PB1, PB2 and PB3 useless for the future formulation in any dosage form.

3.3. Determination of metal composition by inductively coupled plasma mass spectrometry (ICP-MS)

The percentage of iron and potassium present in the all PB compared in this work have been determined by ICP-MS. In Table 2, the observed iron and potassium contents are compared to the expected contents, calculated from the stoichiometry of the insoluble $Fe_4[Fe(CN)_6]_3 \cdot xH_2O$ PB, in which the water content is different. By using EA and TGA, the water content was estimated for each PB. For example, for PB standard, both EA and TGA indicate that the water content is PB is in the range 17–18 molecules. These results indicate that theoretically PB standard contains 335,549 mg/kg of iron. However, the content of iron determined by ICP-MS is around 9 % less than the theoretical one. These results indicated again that the exact content of water or hydration, which is often difficult to determine, will have an important impact on the calculated amount of iron and potassium present in the sample. The presence of potassium in all analyzed samples can be explained due to the tendency of PB to introduce metal inside of its lattice. The ratio of K/Fe in PB standard is 2.38 % whereas as in the PB test represents 5.8 %. This percentage does not correspond to the ratio K/Fe present in soluble PB, confirming the presence only the insoluble PB species.

3.4. Scanning Electronic Microscopy (SEM)

The images of PB test and PB standard recorded by electron microscope indicate that the PB present a crystalline morphology with a smooth surface with great variability in particle size and length (Fig. 4). Moreover, the sizes of the crystals in the PB standard sample are higher compared to those achieved in the locally manufactured raw material, which represents an advantage from the technological point of view to produce tablets.

The SEM images in Fig. 4 showed that the morphology of the crystals in both samples could be considered as equivalent. In the 400X

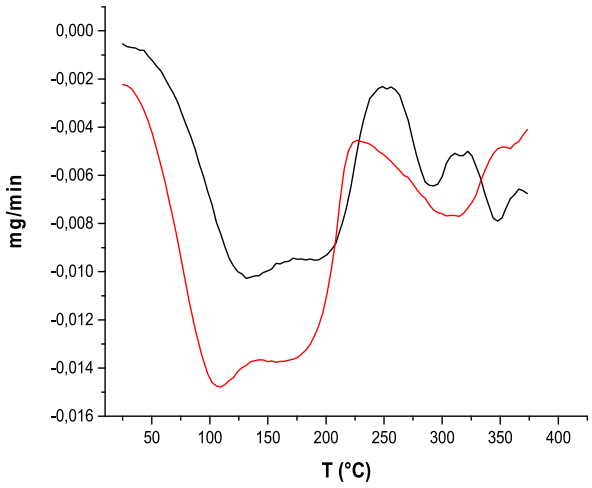

Fig. 2. TGA curves of PB Radiogardase (®) (black line) and PB test (red line).

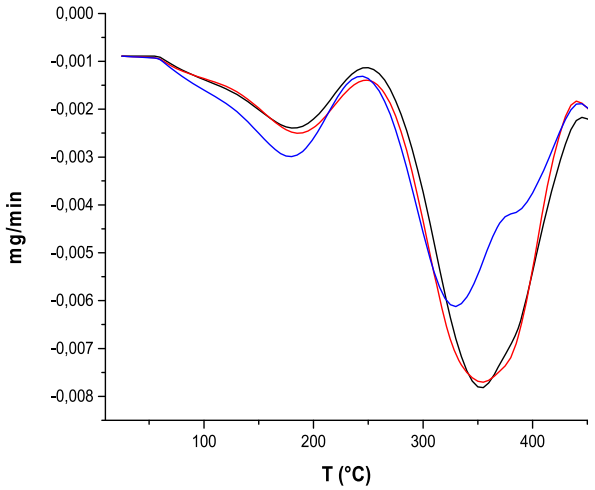

Fig. 3. TGA curves of commercially available PBs. First derivate PB1 (red line), PB2 (blue line) and PB3 (black line).

Table 2
Determination of PB's water content, formula, and molecular weight by TGA.

H_2O content (%)				MW (g/mol)	mg/kg		
Reference	**Zeolitic**	**Coordination**	**Molecular Formula**		**mg**	**K**	**Fe**
PB1	3.47	2.72	Fe_4 $[Fe(CN)_6]_3 \cdot 3H_2O$	913	322 ± 0.7	1342 ± 0.9	344,000 ± 1.9
PB2	4.98	2.72	Fe_4 $[Fe(CN)_6]_3 \cdot 4H_2O$	931	544 ± 1.1	1790 ± 1.5	344,000 ± 0.7
PB3	3.57	2.58	Fe_4 $[Fe(CN)_6]_3 \cdot 3H_2O$	913	322 ± 0.7	1538 ± 0,9	343,000 ± 1.9
PB Standard	15.63	10.96	Fe_4 $[Fe(CN)_6]_3.18H_2O$	1165	N.D.	7120 ± 4.7	299,000 ± 2.2
PB test	21	10.63	Fe_4 $[Fe(CN)_6]_3.22H_2O$	1255	N.D.		

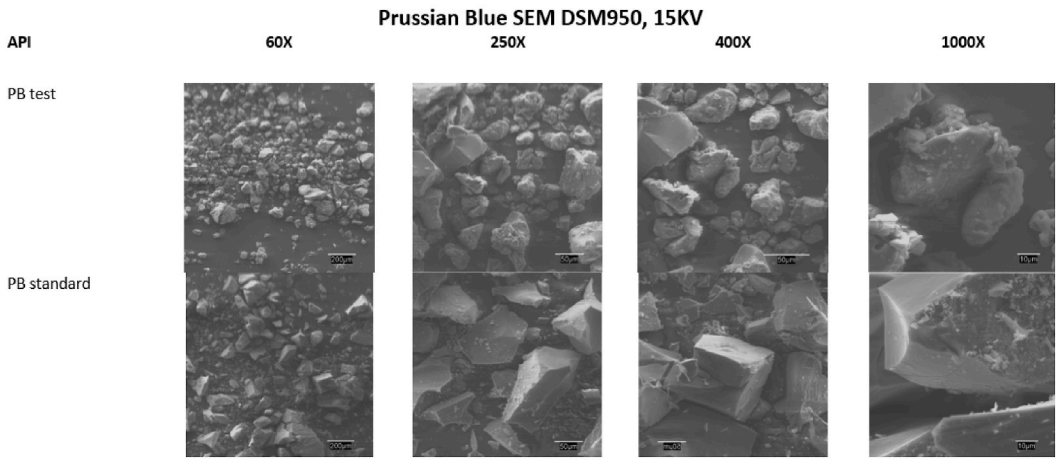

Fig. 4. Electronic images of PB test and PB standard.

magnification it is seen that the PB crystallizes predominantly in cubic form. The 60X magnification showed that the particles did not have in either case a tendency to form aggregates. All images revealed submicron particles.

3.5. Particle size distribution studies (PSDs)

The characterization studies of the size and distribution of the particles of the ingredients of a pharmaceutical formulation are considered valuable information, since their pharmacotechnical and physicochemical behavior depends to a great extent on these values, at each stage of formulation development, from the laboratory scale to industrial level production.

At it is shown in Table 3, the PB test presents a more uniform and lower value of particle size on average (257 μm) than the PB

standard (336 μm), maintaining an equivalent particle size distribution that allows both the flow of the material and the suitable mixing processes, considering the particle sizes of the possible excipients to be used. These results are in agreement which those obtained by electronic microscope.

If the particles of a solid are smaller, the surface area increases, this increase in the surface area is of great interest, since the zeolitic behavior of PB only take place in the surface of the crystalline network, therefore, the higher the surface area is related with an increase of the decorporant capacity [4].

On the other hand, the efficiency with which the particles are compressed, that is, the compression density, is crucial for the manufacture of solid dosage forms. As a rule, large particles compress less than small particles. By reducing the size of the particles, the compression density is improved, and voids (unoccupied volume) are reduced. This is especially relevant in the production of tablets to avoid flaking and percentages of friability out of specifications [38,39].

3.6. Angle of repose determination

For the evaluation of the results obtained in the angle of repose determination for PB and to stablish its flow properties, the values recorded in Table 4 were used as reference.

The repose angle measured for PB test was 34.8 ± 0.6°. This result indicates that the locally synthesized PB indicates has good flow properties. This is a fact that is also confirmed by the sliding time/flow time of the material, which is less than 1 s, determined in triplicate by the falling time of material in the angle of repose test.

A combination of good values for flow time, <1 s, and the angle of repose between 31 and 35° confirm the good flow properties of locally manufactured PB, which emerge due to the particle size, the absence of electrostatic charges and the crystalline properties of the product.

These flow properties are critical as the active ingredient constitutes a high % of the formulation (71.43 %). These results indicate that in the future selection of excipients for a PB tablet formulation the addition of glidants will not require a special effort, because the active ingredient has good flowability and is expected to represent a good proportion within the tablet ingredients. On the other hand, the need to include excipients that favor compressibility and disintegration may be detrimental to the good fluidity of PB crystals, provided that the size is not decreased too much, in which case these properties would be impaired.

3.7. Differential Scanning Calorimetry (DSC)

The DSC thermograms of PB Standard and PB test show the presence only of one endothermic peak corresponding to the melting t™rature (Tm) at 168.51 °C and 172.85 °C, respectively. These two temperatures differ only in less than 5 °C. The molar enthalpy of melting (ΔHm) was also calculated for each PB, being 174.3 J/g and 130.2 J/g, at a constant heating rate of 5 °C/min, respectively (Fig. 5). At it is shown in Fig. 5, both thermograms are very similar and the presence of a flat baseline in both cases suggested the absence of phase transitions. These results indicate that both PB samples are equivalent, and that they do not correspond to polymorphic modifications or different crystalline forms, as expected.

At the same time, the thermal behavior of both commercial PBs (PB1 and PB2) was also evaluated. By using the same experimental conditions implemented for PB standard, the DSC analysis indicated that both, PB1 and PB2, highly differs from the Tm and ΔHm of PB standard (Figs. 6 and 7). The Tm and ΔHm values calculated for PB1 were 192.78 °C and 55.49 J/g, respectively. However, the values obtained for PB2 were higher than those obtained for PB standard, being the Tm of 210.09 °C and ΔHm of 71.08 J/g.

These results indicate that both commercial PB samples are different from PB standard and thus, from PB test, and that they may correspond to polymorphic modifications or different crystalline forms.

3.8. Fourier Transform Infrared Spectrophotometry (FTIR)

All the PBs employed in this study were characterized by the InfraRed (Fig. 8). The InfraRed spectra of PB test and PB standard show a broad band around 3400 cm^{-1} which is characteristic of O–H group of crystallized or zeolitic water. In both cases, it is observed absorption peak at 3630 cm^{-1}, which is characteristic of the coordinate water. Around 2000 cm^{-1} appears the characteristic band of the metal coordinated C–N bonds [50]. The characteristic band for C–N is very wide in both cases, possibly due to the electronic delocalization generated by the coordination structure of which it is part. It should be noted that the behavior of the PB test corresponds to that of the PB used as standard.

The main difference between the commercial PB1 and PB2 and standard and test PBs is the intensity of the C–N band. This value can

Table 3
Distribution of Particle size of analyzed PBs.

Reference	Dv (10) μM	Dv (50) μM	Dv (90) μM	[4:3]μM
PB1	15.6	69.3	177	86.4
PB2	25.7	76.5	210	101
PB3	37.7	95.2	215	114
PB standard	49.8	315	662	336
PB test	59.0	213	495	257

Table 4
Flow properties and correspondent repose angles [44,49].

Repose angle (°)	Flow Properties
25–30	Excellent
31–35	Good
36–40	Correct
41–45	Tolerable
46–55	Poor
56–65	Very poor
>66	Very, very poor

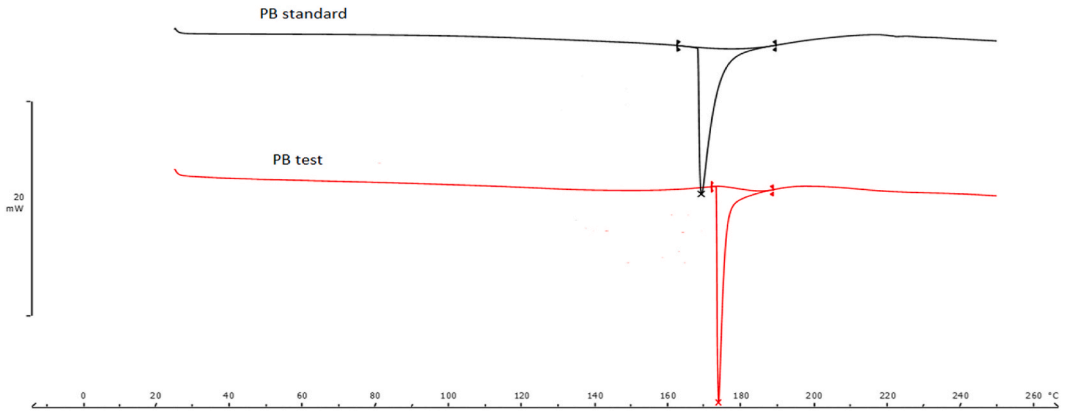

Fig. 5. Thermograms of PB standard and PB test.

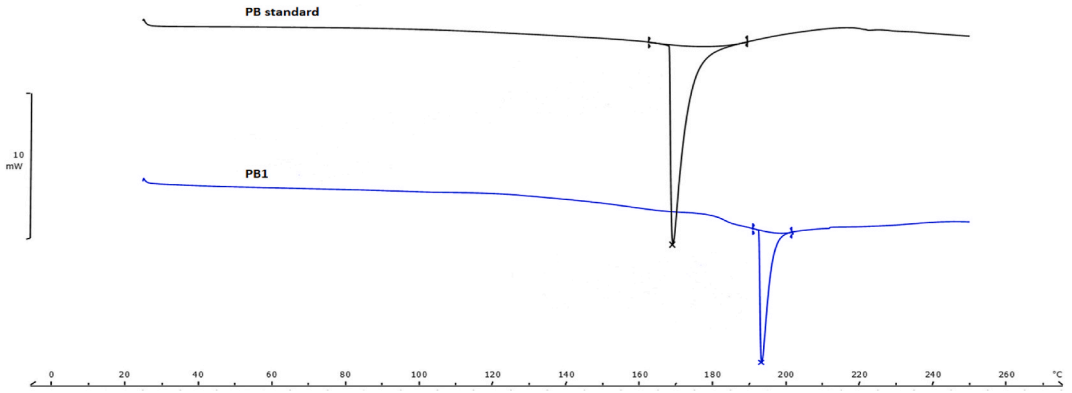

Fig. 6. Thermograms of PB standard and PB1.

be interpreted as a major amount of CN groups in these two compounds.

3.9. X-ray diffraction (XRD)

In the evaluation by X-ray diffractometry, the most distinctive signals are evaluated, which are those that pro-vide the information presented in Fig. 9.

A comparison of both diffractograms obtained by XRD for PB test and PB standard indicate that they are equivalent, revealing a similar degree of crystallinity due to both the absence of displacement of the absorption peaks, and the degree of intensity of the peaks. The highest values correspond to the sample compared to the standard.

The previous results are in agreement with those found in the FIR and DSC studies.

Finally, the XRD studies confirm the crystallinity of PB test and the one used as a standard. Despite the small differences in their degree of crystallinity, it can be considered that the locally produced PB sample corresponds to the one used as a standard. The XRD study allows us to affirm that they have an equivalent degree of crystallinity, based on the distinctive signals, and the absence of

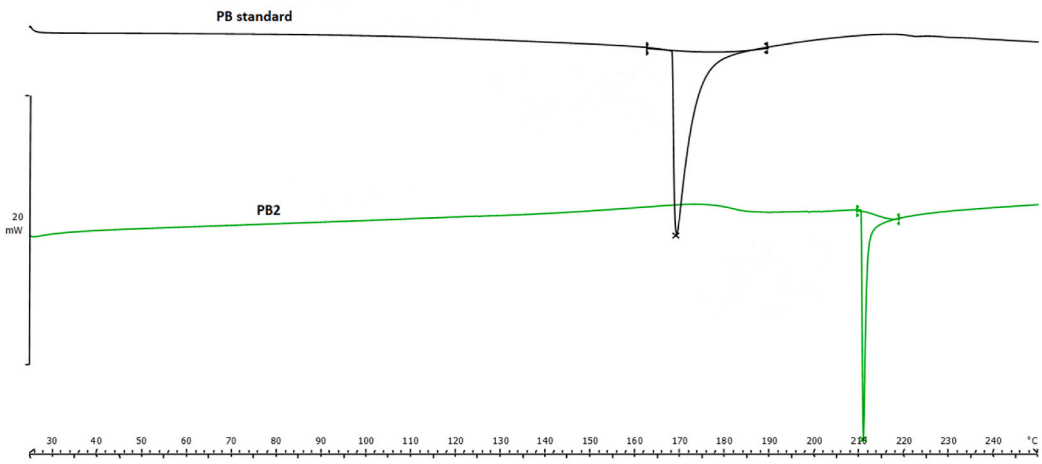

Fig. 7. Thermograms of PB standard and PB2.

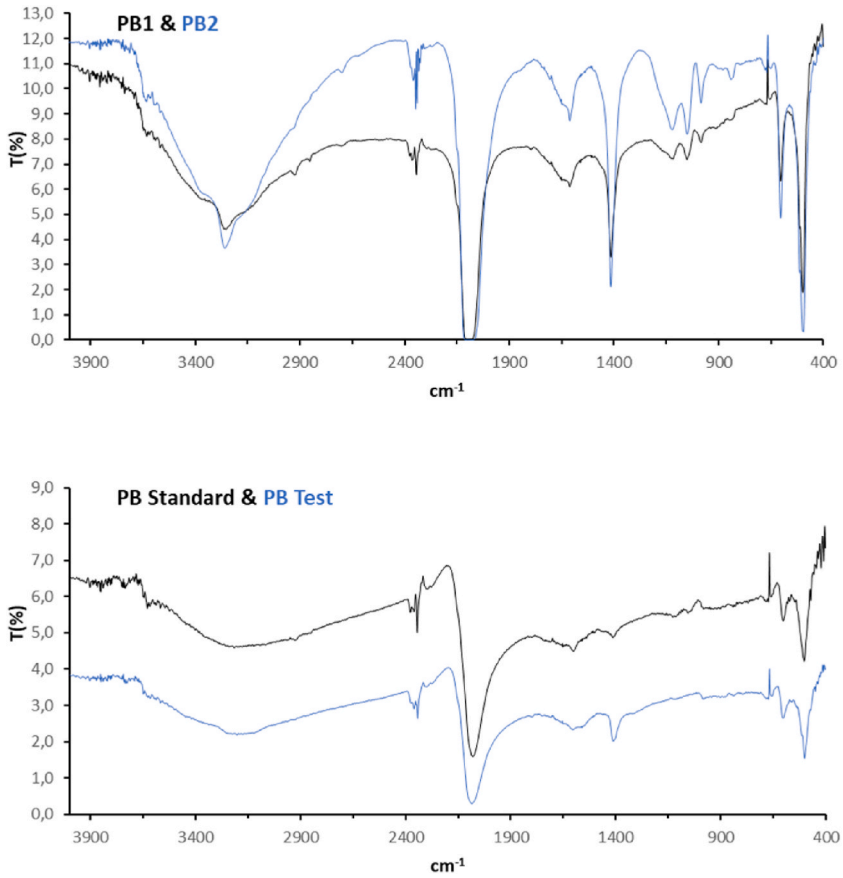

Fig. 8. FTIR spectra of all insoluble PB samples.

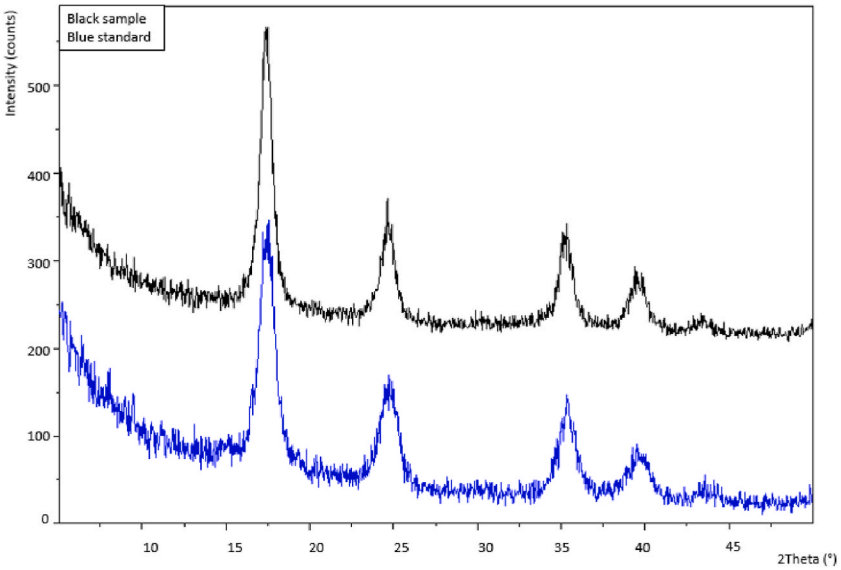

Fig. 9. X-ray diffractograms of PB.

displacement. On the other hand, the influence on the decorporating capacity detected by the slight differences due to its fragility should be evaluated in subsequent studies.

3.10. Determination of Cs binding capacity at pH 7.4 for 24 h (600 ppm)

As it was mentioned before, the binding of radioactive Cs to insoluble PB is affected by the pH value displaying a pH-dependent profile with an increase of the binding with increases of pH [48]. Moreover, it is also described that the maximum binding is reached at pH 7.5 [9]. Moreover, these authors showed that the binding equilibrium is adopted after 24 h. Due to these facts, pH 7.4–7.5 was selected to determine the Cs binding capacity of all the PB samples using Cs concentration of 600 ppm for 24 h.

At it is shown in Fig. 10, the lowest amount of Cs binding occurred for PB1, PB2 and PB3 ranging from 53 to 113 mg Cs/gram of Prussian Blue. Whereas the highest amount of Cs binding was found for PB standard and PB test, being 415 and 428 mg Cs/g PB, respectively.

These results indicated that the hydration stage of PB has a strong influence on the Cs binding process, existing a direct correlation between them. In general terms, the loss of moisture reduces the binding capacity, indicating that the water molecules in PB are involved in Cs and PB interaction. Thus, in the cases of PB1, PB2 and PB3 with only 4 to 6 water molecules have lest binding capacity PB standard and PB test, in which the number of water molecules are 18 and 22, respectively.

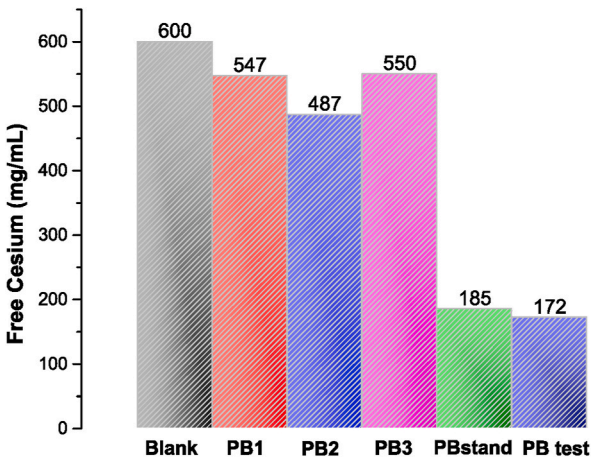

Fig. 10. Comparison of Cs binding capacity sample to sample of PB. Each sample was incubated with 600 ppm Cs in phosphate buffer solution of 40 mM with pH 7.4 at 37 °C for 24 h.

3.11. Concentration dependent profile. Determination of maximal binding capacity (MBC)

After the last experiment, only the PB standard and PB test were selected to determine the maximal binding capacity (MBC) to Cs at pH 7.4. For this purpose, different Cs concentrations ranging from 300 to 1800 ppm were used and taking into account that the Cs binding acquires the equilibrium at 24 h (Fig. 11). After that, the obtained data at this time were used for plotting the Langmuir isotherm (Fig. 12). In the Langmuir equation:

$$C_{xm} = \frac{1}{k_1 k_2} + \frac{C}{k_2}$$

Cxm is the ratio of free to bound Cs, C oncentrationCs concentratio in mg/L, k1 is the affinity constant, and k2 is the MBC in mg of Cs/g of PB, calculated from the slope (1/k2) using least squares linear regression.

As it is shown in Fig. 11, the binding Cs capacity of both PB is very similar and it related with the Cs concentration. At 300 ppm, the amount of Cs binding to both PB is around 200 mg Cs/g PB. However, this amount is increased when increase the Cs concentration. The highest amount of Cs binding to PB test was 501 mg Cs/g PB at 1500 ppm compared to 217 g Cs/g PB at 300 ppm. The PB standard has similar behavior binding the highest Cs amount of 495 mg Cs/g PB at 1800 ppm.

From the Langmuir isotherm and considering the calculated slope (1/k2) in this study, the MBC was found to be approximately 561 mg Cs/g PB for PB test and 578 mg Cs/g PB standard, respectively (Fig. 12).

4. Conclusions

It can be said from the results of Studies of Elemental Analysis (EA), Scanning Electronic Microscopy (SEM), Laser Diffraction Technology for Measuring Particle Size Distributions (PSDs), Differential Scanning Calorimetry (DSC), Fourier Transform Infrared Spectrophotometry (FTIR), Thermogravimetric Analysis (TGA) and X-Ray Diffraction (XRD) performed following the Real Farmacopea Española recommendations for this techniques, that the PB obtained locally is equivalent in every single aspect evaluated to the commercially available standard PB. Moreover, these analytical techniques allow to distinguish the insoluble and approved form of PB from those other chemical forms which are not authorized, this leads to stablish the need to carry out exhaustive controls to determine the nature of the product and ensure that is the insoluble form of PB authorized for use as a decorporant of radioactive metals. This information together with the extra analysis which confirm that the PB test and PB standard have the same behavior as a decorporant agent, displaying an MBC of 561 and 578 mg Cs/g PB, respectively. However, the commercially available PB1, PB2 and PB3 do not show equal properties indicating that the moisture loss in PB has a strong influence on the decorporation mechanism of action.

These results are of great significance, in combination with the information obtained from the results of pharmacotechnical studies, such as the repose angle determination and flow time, to foresee that the locally developed PB will have an excellent behavior in the formulation of oral dosage forms, like tablets or capsules; decreasing the amount and variety of excipients that will be needed and simplifying the operations in the future production of a drug with PB as an active ingredient. This fact will be considered in the future because it will contribute to improve the conventional release and develop a new oral dosage formulation to improve its efficacy. The incoming development of new PB oral dosage formulation will require deep investigation for an optimal composition selection, characterization and assurance of its quality properties, both right after production, and in long term conducted stability studies following ICH and drugs agencies recommendations. Moreover, these results also contribute to have a new supplier of this costly active principle that are capable of covering the demand for the product for the industrial scale production of the drug, can be validated.

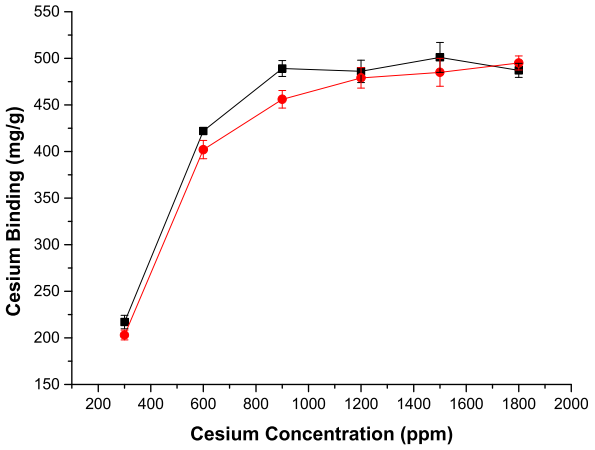

Fig. 11. Concentration dependent profile of PB standard (red line) and PB test (black line). Both PB were incubated with 300, 600, 900, 1200, 1500 and 1800 ppm Cs pH 7.54 at 37 °C for 24 h.

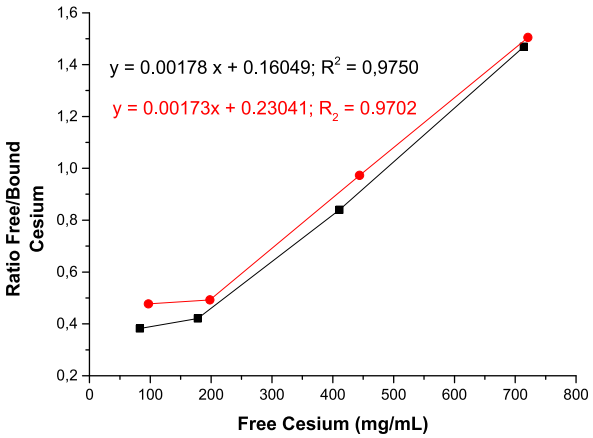

Fig. 12. The concentration – dependent Cs binding profile of PB test (black line) and PB standard (red line). Thus, the Langmuir isotherm for each PB was plotted on 24 h binding data. Linear regression using the least squares method. The X axis represents t.

Funding sources

This research was funded by the Subdirección General de Planificación, Tecnología e Innovación (SDG PLATIN) del Ministerio de Defensa, Gobierno de España.

Data availability

Data will be made available on request.

CRediT authorship contribution statement

Borja Martínez-Alonso: Writing - review & editing, Writing - original draft, Validation, Software, Methodology, Investigation, Formal analysis, Data curation, Conceptualization. **Norma S. Torres Pabón:** Validation, Methodology, Formal analysis. **María Isabel Fernández-Bachiller:** Writing - original draft, Validation, Software, Methodology, Investigation, Formal analysis, Data curation, Conceptualization. **Guillermo Torrado Durán:** Writing - review & editing, Supervision, Resources, Project administration, Investigation, Conceptualization. **Rocío González Crespo:** Validation, Data curation. **Carlos F. Torrado-Salmerón:** Investigation, Formal analysis. **Antonio Juberías Sánchez:** Resources, Project administration. **M. Ángeles Peña Fernández:** Writing - review & editing, Supervision, Investigation, Conceptualization.

Declaration of competing interest

The authors declare the following financial interests/personal relationships which may be considered as potential competing interests: This research received financial support from Government of Spain Ministry of Defense.

References

[1] W. Li, C. Han, G. Cheng, S. Chou, H. Liu, S. Dou, Chemical properties, structural properties, and energy storage applications of Prussian blue analogues, Small 15 (2019).
[2] R.E. Albert, R.E. Train, E. Anderson, Rationale developed by the environmental protection agency for the assessment of carcinogenic risks, J. Natl. Cancer Inst. 58 (1977).
[3] E.L. Anderson, Quantitative approaches in use to assess cancer risk, Risk Anal. 3 (4) (1983) 277–295.
[4] S. Hajat, M. O'Connor, T. Kosatsky, Health effects of hot weather: from awareness of risk factors to effective health protection, Lancet 375 (2010).
[5] J. Hawker, N. Begg, R. Reintjes, K. Ekdahl, O. Edeghere, J.E. van Steenbergen, Comunicable Disease Control and Health Protection Handbook, fourth ed., Wiley Blackwell, Pondicherry, India, 2019.
[6] B.A. Betthäuser, A.M. Bach-Mortensen, P. Engzell, A systematic review and meta-analysis of the evidence on learning during the COVID-19 pandemic, Nat. Human Behav. 7 (2023) 375–385.
[7] E.L. Anderson, P. Turnham, J.R. Griffin, C.C. Clarke, Consideration of the aerosol transmission for COVID-19 and public health, Risk Anal. 40 (2020).
[8] A. Murphy, D. Fuhr, B. Roberts, C.I. Jarvis, A. Tarasenko, M. Mckee, The health needs of refugees from Ukraine, BMJ 377 (2022).
[9] N.R. Haddaway, T. Lotfi, L. Mbuagbaw, Systematic reviews: a glossary for public health, Scand. J. Publ. Health 51 (2023).
[10] K. Wabnitz, E. Schwienhorst-Stich, F. Asbeck, C.S. Fellmann, S. Gepp, J. Lebert, N.C.S. Mezger, M. Eichinger, National Planetary Health learning objectives for Germany: a steppingstone for medical education to promote transformative change, Publ. Health 10 (2022).
[11] M. Kastl, A. Giussani, E. Blanchardon, B. Breustedt, P. Fritsch, C. Hoeschen, M.A. Lopez, Developing a physiologically based approach for modeling plutonium decorporation therapy with DTPA, Int. J. Radiat. Biol. 90 (2014) 1062–1067.
[12] T. Yan, G. Lin, M. Wang, A. Lamkowski, M. Port, A. Rump, Pharmacological treatment of inhalation injury after nuclear or radiological incidents: the Chinese and German approach, Mil. Med. Res. 6 (2019) 10.

[13] D. Parajuli, H. Tanaka, Y. Hakuta, K. Minami, S. Fukuda, K. Umeoka, R. Kamimura, Y. Hayashi, M. Ouchi, T. Kawamoto. Dealing with the aftermath of Fukushima daiichi nuclear accident: decontamination of radioactive cesium enriched ash. Environ. Sci. Technol.. 47 82013) 3800-3806..

[14] K.O. Buesseler, S.R. Jayne, N.S. Fisher, I.I. Rypina, H. Baumann, Z. Baumann, C.F. Breier, E.M. Douglass, J. George, A.M. Macdonald, H. Miyamoto, J. Nishikawa, S.M. Pike, S. Yoshida, Fukushima-derived radionuclides in the ocean and biota off Japan, Proc. Natl. Acad. Sci. U.S.A. 109 (2012) 5984–5988.

[15] P. Dubé, S. Gosselin, Prussian blue, in: J. Brent, P. Burkart, B. Hatten, R. Palmer, J. White (Eds.), Critical Care Toxicology, Springer, Cham, 2017, pp. 2957–2962.

[16] S. Jang, S. Hong, H. Yang, K. Lee, J. Moon, B. Seo, Y.S. Huh, C. Roh C, Removal of radioactive cesium using Prussian blue magnetic nanoparticles, Nanomaterials 4 (2014) 894–901.

[17] Agencia para Sustancias Tóxicas y el Registro de Enfermedades Resumen de Salud Pública Cesio CAS#: 7440-46-2, División de la Toxicología abril de 2004, 2016.

[18] P.J. Faustino, Y. Yang, J.J. Progar, C.R. Brownell, N. Sadrieh, J.C. May, E. Leutzinger, D.A. Place, E.P. Duffy, F. Houn, S.A. Loewke, V.J. Mecozzi, C.D. Ellison, M. A. Khan, A.S. Hussain, R.C. Lyon, Quantitative determination of cesium binding to ferric hexacyanoferrate: prussian blue, J. Pharmaceut. Biomed. 47 (2008) 114–125.

[19] J. Zan, Z. Zhang, M. Dou, F. WangF, Prussian blue nanocubes decorated on nitrogen-doped hierarchically porous carbon network for efficient sorption of radioactive cesium, J. Hazard Mater. 385 (2020) 121568.

[20] P.J. Faustino, A. Brown, B. Lowry, Y. Yang, Y. Wang, M.A. Khan, K.R. Dunbar, A. Mohammad. Quantitative evaluation of the thallium binding of soluble and insoluble Prussian blue hexacyanoferrate analogs: a scientific comparison based on their critical quality attributes. Int. J. Pharmacol.. 569 82019) 118600..

[21] S. Li, W. Huang, Y. Duan, J. Xing, Y. Zhou, Human fatality due to thallium poisoning: autopsy, microscopy, and mass spectrometry Assays, J. Forensic Sci. 60 (2015) 247–251.

[22] C.A. Foradori, IV Los efectos biológicos de las radiaciones ionizantes, Ars. Med. 19 (2017) 33–39.

[23] D.R. Melo, J.L. Lipsztein, R. Leggett, L. Bertelli, R. Guilmette. Efficacy of Prussian blue on 137Cs decorporation therapy. Health Phys. (Tokyo)s. 106 82014) 592-597..

[24] J. Pearce, Studies of any toxicological effects of Prussian blue compounds in mammals—a review, Food Chem. Toxicol. 32 (1994) 577–582.

[25] M.A. Miller, M.M. Patel, T. Coon, T. Prussian blue for treatment of thallium overdose in the US. Hosp. Pharm.. 40 82005) 796-797..

[26] V.K. Singh, M. Garcia, S.Y. Wise, T.M. Seed, Medical countermeasures for unwanted CBRN exposures: Part I chemical and biological threats with review of recent countermeasure patents, Expert Opin. Ther. Pat. 26 (2016).

[27] V.K. Singh, P.L.P. Romaine, V.L. Newman, T.M. Seed, Medical countermeasures for unwanted CBRN exposures: part II radiological and nuclear threats with review of recent countermeasure patents, Expert Opin. Ther. Pat. 26 (2016).

[28] T. Yan, G. Lin, M. Wang, A. Lamkowski, M. Port, A. Rump, Pharmacological treatment of inhalation injury after nuclear or radiological incidents: the Chinise and German approach, Military Medical Research 6 (2019).

[29] R.A. Guilmette, B.A. Muggenburg. Decorporation therapy for inhaled plutonium nitrate using repeatedly and continuously administered DTPA. Int. J. Radiat. Biol.. 63 81993) 395-403..

[30] J. Wang, S. Zhuang, Y. Liu, Metal hexacyanoferrates-based adsorbents for cesium removal, Coord. Chem. Rev. 374 (2018) 430–438.

[31] M. Altagracia, M, J. Kravzov, J.M. Martínez, C. Ríos, F. López, Prussian blue as an antidote for radioactive thallium and cesium poisoning, Orphan Drugs Res. Rev. 2 (2012) 13.

[32] H.J. Buser, D. Schwarzenbach, W. Petter, A. Ludi, The crystal structure of Prussian Blue: Fe4[Fe(CN)6]3·xH2O, Inorg. Chem. 16 (1977) 2704.

[33] J.W. Runge, B.R. Buddemeier, Explosiones y material radiactivo: una introducción dirigida a los profesionales de primera respuesta, Prehosp. Emerg. Care 3 (2010) 63–80.

[34] A. Rump D. Stricklin, A. Lamkowski, S. Eder, M. Abend, M. Port. Reconsidering decorporation strategies after the incorporation of radionuclides. Health Phys. (Tokyo)s. 111 82016) 201–208..

[35] A. Rump, D. Stricklin, A. Lamkowski, S. Eder, M. Abend, M. Port, Analysis of the antidote requirements and outcomes of different radionuclide decorporation strategies for a scenario of a “dirty bomb” attack, Am. J. Disaster. Med. 12 (2017) 227–241.

[36] D.F. Thompson, E.D. Callen, Soluble or insoluble prussian blue for radiocesium and thallium poisoning? Ann. Pharmacother. 38 (2004) 1509–1514.

[37] S. Manabe, V. Adavan, T. Kumashiro, S. Takiguchi, B. Fugetsu, I. Sakata, Stabilization of Prussian blue using copper sulfate for eliminating radioactive cesium from a high pH solution and seawater, J. Hazard Mater. 386 (2020) 121979.

[38] M. Sayalero, C. Maderuelo, Formas farmacéuticas orales de liberación inmediata, in: R. Martínez (Ed.), Tratado de tecnología farmacéutica. Volumen III, Formas de dosificación, first ed., Síntesis, Madrid, Spain, 2017.

[39] A. Concheiro, Formas de dosificación de medicamentos: concepto, funciones y clasificación, in: R. Martínez (Ed.), Tratado de tecnología farmacéutica. Volumen III, Formas de dosificación, first ed., Síntesis, Madrid, Spain, 2017.

[40] R. Chadha, B.S. Swati, Drug–excipient compatibility screening. Role of thermoanalytical and spectroscopic techniques, J. Pharm. Biomed. Anal. 87 (2014) 82–97.

[41] T.V. Sachin, N.M. Deodhar, V. Prakya, Advances in analytical techniques used in predicting drug-excipient interactions, Int. J. Pharm. Technol. 6 (2014) 6388–6417.

[42] L. Samain, F. Grandjean, G.J. Long, P. Martinetto, P. Bordet, D. Strivay, Relationship between the synthesis of prussian blue pigments, their color, physical properties, and their behavior in paint layers, J. Phys. Chem. 117 (2013) 9693–9712.

[43] Vademecum, Available online: https://www.vademecum.es/equivalencia-lista-radiogardase+gelule+500+mg-francia-v03ab31-170366-fr_1. (Accessed 1 April 2023).

[44] 2.9.16 Capacidad de flujo, in: Real Farmacopea Española, sixth ed., Ministerio de Sanidad y Consumo, Madrid, Spain, 2023.

[45] B.C. Pereira, A. Isreb, R.T. Forbe, F. Dores, R. Habashy, J.B. Petit, M.A. Alhanan, E.F. Oga, A novel solution to fabricate 3D printed patient-centred cardiovascular “Polypill” architectures, Eur. J. Pharm. Biopharm. 135 (2019) 94–103.

[46] N. Ruankaew, N. Yoshida, Y. Watanabe, H. Nakano, S. Phongphanphanee. Size-dependent adsorption sites in a Prussian Blue nanoparticle: a 3D-RISM study. Chem. Phys. Lett.. 684 82017) 117-125..

[47] M. Ishizaki, S. Akiba, A. Ohtani, Y. Hoshi, K. Ono, M. Matsuba, T. Togashi, K. Kanaizuka, M. Sakamoto, A. Takahashi, T. Kawamoto, H. Tanaka, M. Watanabe, M. Arisaka, T. Nankawa, M. Kurihara, Proton-exchange mechanism of specific Cs+adsorption via lattice defect sites of Prussian blue filled with coordination and crystallization water molecules, Dalton Trans. 42 (2013) 16049–16055.

[48] A. Mohammad, Y. Yang, M.A. Khan, P.J. Faustino, Long-term stability study of Prussian blue — a quality assessment of water content and cyanide release, Clin. Toxicol. 53 (2015) 102–107.

[49] C. Civera, M. Córdoba, Reología de materias primas de uso farmacéutico, in: Manual de tecnología farmacéutica, first ed., Elsevier, 2012.

[50] C.M. Pharr, P.R. Griffiths, Infrared spectroelectrochemical analysis of adsorbed hexacyanoferrate species formed during potential cycling in the ferrocyanide/ferricyanide redox couple, Anal. Chem. 69 (1997) 4673–4679.